Analysis of Hydrothermal Ageing on Mechanical Performances of Fibre Metal Laminates

Costanzo Bellini *, Vittorio Di Cocco, Francesco Iacoviello , Larisa Patricia Mocanu, Gianluca Parodo ,
Luca Sorrentino and Sandro Turchetta

Department of Civil and Mechanical Engineering, University of Cassino and Southern Lazio, Via G. Di Biasio 43,
03043 Cassino, Italy
* Correspondence: costanzo.bellini@unicas.it

Abstract: Fibre Metal Laminates (FMLs) are very interesting materials due to their light weight coupled with their high stiffness, high fatigue resistance, and high damage tolerance. However, the presence of the polymeric matrix in the composite layers and of polymeric adhesive at the metal/composite interface can constitute an Achille's heel for this class of materials, especially when exposed to a hot environment or water. Therefore, in the present article, aluminium/carbon fibre FML specimens were produced, aged by considering different hydrothermal conditions, and then, subjected to mechanical testing. The End-Notched Flexure (ENF) test was considered for this activity. It was found that the first ageing stage, consisting of submersion in saltwater, was very detrimental to the specimens, while the second stage, composed of high and low temperature cycles, showed an increase in the maximum load, probably due to a post-curing effect of the resin during the higher temperatures of the ageing cycles and to the dissolution of salt crystals during the subsequently ageing stages in distilled water.

Keywords: fibre metal laminates; hydrothermal ageing; end-notched flexure test

1. Introduction

Structural applications in advanced fields, such as aeronautics, demand innovative materials presenting high mechanical properties, low density, and resistance against ageing. In fact, the mechanical properties of structural parts have to remain unaltered throughout the entire lifecycle, even if the part is exposed to hazardous environments [1]. Fibre Metal Laminates (FMLs) are a class of materials able to meet the aforementioned properties. In fact, they are formed by metal sheets alternated with Fibre-Reinforced Polymer (FRP) layers, and this confers to the material the desired mechanical characteristics [2,3]. From a historical point of view, FMLs were developed to overcome the poor fatigue resistance of aluminium sheets [4,5]. Moreover, FRPs suffer a decrease in mechanical properties due to exposure to water/moisture environments, which are able to damage the matrix of the composite layers [6,7]. In fact, the matrix of FRP generally is hydrophilic. This leads to a tendency for the material to absorb moisture from the outside to the inside. Generally, the mechanisms by which this occurs are essentially two: volumetric and "interaction" [8]. In the first mechanism, the absorption of water in free volumes and microcavities that are present in the FRP such as micro-voids and pores due to gases generated during the polymerisation of the resin throughout the curing process is considered the cause. These gases could remain entrapped in the matrix, increasing the void content in the FRP. In the second mechanism, there is an interaction between the water molecules and the polar groups present in the molecular structure of the polymer. This interaction not only allows diffusion within the polymer, but also involves a plasticisation of the polymer itself as a weakening of the primary and secondary bonds of the molecular structure and distortions of the molecular chains. This phenomenon results in a change in the thermomechanical characteristics of the polymer, which are usually manifested by a reduction in the glass transition temperature

(Tg). On the other hand, thermal ageing is strongly linked to the Tg of the resin used for the production of FRP. Generally, when the temperature of the environment exceeds the Tg of the resin, its mechanical characteristics undergo a strong reduction, which can be recovered if the working temperature is reduced below the Tg. However, such temperature changes affect the molecular structure by generating configuration changes [9]. However, the effects of physical ageing related to the presence of moisture in the polymer or the presence of high-temperature environments can be recovered if chemical degradation of the molecular bonds does not occur. In fact, if a polymer is exposed for a certain time to a temperature close to its Tg, its aging history is lost. For epoxy resins, this phenomenon can also occur at temperatures lower than the Tg, definable as erasure temperatures [10].

The presence of the metal sheets on the exposed surface of the laminate is able to reduce the penetration of moisture into the FRP resin [11]. For this reason, FMLs can be employed in environments characterised by intense temperature variations and elevated humidity [12]. However, ageing can affect the mechanical properties of the FML, leading to dangerous delaminations in the laminate and, consequently, to its failure [13]. Moreover, the presence of an interface could accelerate the moisture uptake in the FML because it can be the most-critical area in terms of mechanical strength and temporal reliability [14].

There are several studies about the mechanical properties of FMLs, paying attention to the composite type [15], the thickness of the layers [16], the metal's surface preparation [17], and the fibre orientation [18]; however, there has not been much research performed on the hygrothermal effects on carbon-based FMLs, and it is still unclear how long layers will stay bonded, particularly in seawater environments or at high temperatures. Yu et al. [14] prepared titanium/Carbon-Fibre-Reinforced Polymer (CFRP) FMLs by anodising the titanium sheets and grafting the CFRP layers with multi-walled carbon nanotubes. Then, they compared the interlaminar fracture toughness of the produced laminates with that of an equivalent, but untreated, one, by considering both as-produced and aged materials. They found much better behaviour for the treated laminate. Instead, Wang et al. [19] studied the effect of graphene nanoplatelets on the impact resistance of FMLs subjected to different hygrothermal ageing conditions, finding that the addition of nanoplatelets decreased the water absorption and increased the impact resistance. Pan et al. [20] investigated the effects of aluminium sheet treatments on the mechanical performances of a hydrothermally aged CFRP FML. They found a greater decrease of the mechanical properties in the untreated laminates, due to the corrosion of the aluminium sheets. Hamill et al. [21] studied the effect of galvanic corrosion induced by ageing in saltwater on traditional aluminium/CFRP FML and an innovative bulk metallic glass/CFRP FML. They found a lower corrosion resistance in the former one, which was reflected in the tensile properties of the materials, while the flexural properties remained unaffected. To reduce the effects of environment-induced galvanic corrosion, Stoll et al. [1] added an elastomeric interlayer between the aluminium sheets and the carbon layers, suitable to reduce the corrosion thanks to its high electrical resistance. They found decreased mechanical properties in the laminate produced without the elastomer. Ali et al. [13] compared the effect of hydrothermally induced corrosion on the mechanical properties of titanium sheets, CFRP laminates, and titanium/CFRP FMLs. They found higher mechanical characteristics in the FML compared to the CFRP laminates, while the titanium sheets presented the lowest corrosion. Viandier et al. [22] studied the corrosion resistance of an FML based on CFRP and stainless steel, finding that the former behaved as a cathode, while the latter as an anode, and it was affected by pitting corrosion as well. Alia et al. [12] studied the effect of hydrothermal ageing on the adhesive layer used for bonding the metal with the composite in the FML, evaluating the diffusion of water throughout the adhesive thickness and finding both microstructural changes and chemical degradation in the latter. Hu et al. [23] compared the effect of moisture absorption on the mechanical behaviour of carbon-fibre-reinforced polyimide and polyimide–titanium-based FMLs. They subjected samples of these materials to a high-temperature and high-relative-humidity environment for different amounts of time, and then, they evaluated the interlaminar shear strength and the flexural strength of the

aged specimens. A certain decrease in these properties was found, induced by ageing, as confirmed also by scanning electron micrographs and dynamic mechanical analysis tests. Hu et al. [24] investigated the effect of hydrothermal ageing on Ti/CF/PMR polyimide composite laminates conditioned in environments at different combinations of temperature and relative humidity. They found that the saturated moisture absorption rate depended on the relative humidity, while the diffusion rate of water in the composite depended on the temperature. Zhang et al. [25] proposed a reduced graphene oxide modified Ti/CFRP laminate to be used for intelligent de-icing in aeroplanes and tested both the de-icing performances and the mechanical properties of this laminate. They found that the mechanical properties improved after several de-icing cycles.

The aim of the present work is to investigate the effect of hydrothermal ageing on the mechanical performances of FMLs. Specimens made of CFRP and aluminium sheets were subjected to a sequence of different environments, such as saltwater, hot water, and ice, as will be better described in the "Materials and Methods" Section. The motivation behind this choice can be explained as the willingness of reproducing the possible environments an aeronautical part is subjected to. Therefore, in the present work, End-Notched Flexure (ENF) specimens were manufactured, aged under different conditions, and finally, tested through a three-point bending scheme in order to analyse the effect of hydrothermal ageing on the bonding interface between metal sheets and composite layers in an FML made of aluminium and CFRP.

2. Materials and Methods

FMLs made of carbon composite laminates and aluminium sheets were chosen for the investigation presented in this work. According to published research, galvanic corrosion affects FMLs made of CFRP and aluminium sheets because the standard electrode potentials of carbon and aluminium differ. Due to this peculiarity, the combination of these materials was chosen since it is extremely important when thinking about the issue of environment-induced corrosion, the goal of this work being to explore the impact of hydrothermal ageing on the mechanical properties. The FMLs considered in this work were manufactured using the prepreg vacuum bag process, as already described in [26]. The metal layers of the produced FMLs were made of EN AW 3105, a commercial aluminium alloy, while the layers of CFRP were made of M92/48%/220H4/AS4C/3K, a woven thermoset prepreg system. The aluminium sheets had a thickness of 0.8 mm, while the prepreg layers had a thickness of about 0.25 mm in the uncured state. The layup sequence is reported in Figure 1. The composite layer consisted of two plies of M92/48%/220H4/AS4C/3K, layered in the roll direction. The composite laminates were co-bonded to the aluminium sheets using the structural adhesive AF 163-2, manufactured by 3M. As the pretreatment for the bonding, the aluminium sheets were degreased using Methyl Ethyl Ketone (MEK). Specifically, the FMLs were made using the vacuum bag technique: the cure cycle consisted of a heat ramp of 2 °C/min up to the temperature of 125 °C and a dwell at this temperature of about 90 min. This thermal cycle was suitable for both the prepreg and adhesive, as reported in the respective technical sheets. Two notches were made using a very thin Polytetrafluoroethylene (PTFE) release film at the interface between the composite and the aluminium inner sheet in order to realise a notch length of about 30 mm in the finished specimens. In fact, once the cure was complete, the laminate was removed from the mould, and ENF specimens were made through a cutting operation using a diamond blade. In particular, the specimen dimensions were determined in accordance with ASTM D7905 [27], as shown in Figure 2. In total, 20 specimens were produced.

Ageing Treatments

To study the behaviour of the hybrid laminate in various types of possible working conditions, five specimens, which represented the reference for measuring the mechanical performance in unaged conditions, were stored in a chamber with a humidity of 30% and a temperature of 25 °C, while the other specimens were subjected to the hydrothermal ageing

cycle reported in Figure 3. It is possible to subdivide the ageing cycle into three stages. Specifically, in the first stage, for a duration of 14 days, the specimens were immersed at room temperature in saltwater with a chemical composition according to ASTM D1141 [28]. For the preparation of saltwater, 2 stocks and a final container were used. In the first stock, 7 L of distilled water was placed and 3889 g of magnesium chloride hexahydrate, 405 g of calcium chloride anhydrous, and 15 g of strontium chloride hexahydrate were dissolved. In the second stock, 486 g of potassium chloride, 141 g of sodium bicarbonate, 70 g of potassium bromide, 19 g of boric acid, and 2 g of sodium fluoride were diluted in 7 L of distilled water. Finally, the preparation of the saltwater was made in the final container. To prepare it, 245 g of sodium chloride and 41 g of sodium sulphate were dissolved in 8 L of water. After, 200 mL of the solution in Stock 1 and 100 mL of the solution in Stock 2 were added to the container. Finally, the obtained solution was diluted with distilled water until a volume of 10 L was reached.

Figure 1. FML layup sequence adopted in this work.
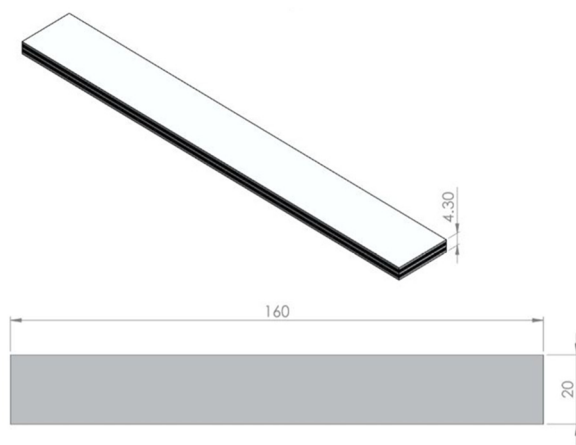
Figure 2. Manufactured ENF specimens: (**a**) geometry and dimensions in mm; (**b**) a photo of a group.

Subsequently, five specimens were extracted and stored in a dry environment at room temperature, while the others were immersed in distilled water and subjected to thermal shocks between -28 °C and 80 °C. Each ageing cycle lasted 7 days, and the thermal variations imposed are illustrated in Figure 4. The adopted ageing cycles simulated the most-critical environments an aeroplane could be exposed to: parking in the snow or ice, near the sealine, and high-altitude flight after a take off from a very hot and sunny location. It is worth pointing out that the edges of the specimens were not sealed in order to procure the most-critical condition for the specimens. In fact, the metal sheet, placed on the external surfaces, protects the FML from moisture and water absorption. By exposing the edges to the environment, the detrimental effects, due to the galvanic coupling between carbon fibres and aluminium sheets, are intensified.
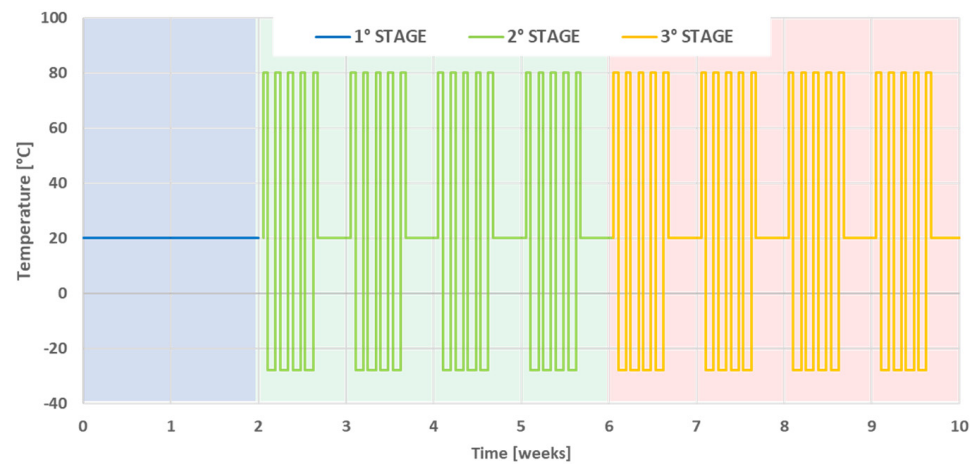
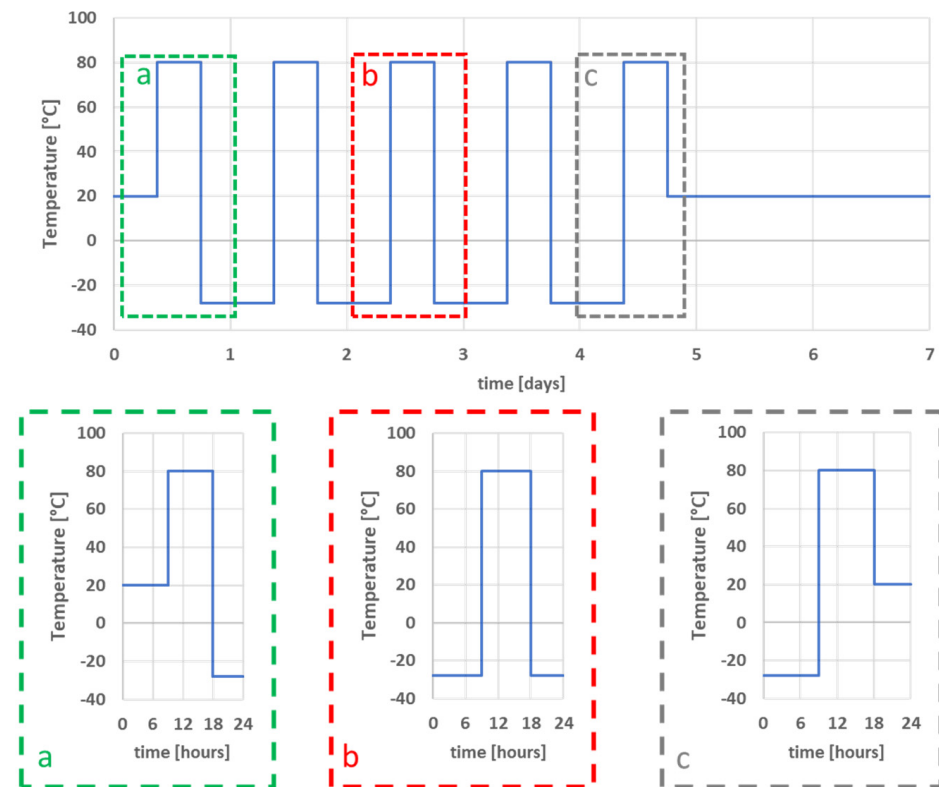**Figure 3.** Hydrothermal ageing cycle adopted in this work.

Figure 4. Temperature variations of specimens immersed in distilled water for one week: (**a**) first day of the week; (**b**) from the second to fourth day; (**c**) fifth day of the week.

After four cycles, five specimens were removed from the distilled water and stored in a dry environment at room temperature. At the end of each ageing stage, the specimens were dried and weighed using a precision balance. Weight variations were calculated only for samples that were subjected to the ageing stages. For each specimen, a coefficient of variation with respect to the unaged condition cwv_{Ref} (defined as the reference weight, which consisted of the weight of the specimen before ageing) was calculated using Equation (1):

$$cwv_{Ref} = \frac{P_{n\ stage} - P_{ref}}{P_{ref}} \tag{1}$$

where $P_{n\ stage}$ is the weight of the specimen after the nth stage, while P_{ref} is the weight of the specimen in unaged conditions. Similarly, it is possible to calculate the coefficient of weight variation with respect to the previous ageing stage cwv_n according to Equation (2):

$$cwv_n = \frac{P_{n\ stage} - P_{n-1\ stage}}{P_{n-1\ stage}} \tag{2}$$

where $P_{n-1\ stage}$ is the specimen weight after the previous ageing stage considered.

Once having completed the ageing treatments, the specimens were stored for two years at room temperature and subsequently subjected to flexural tests. These tests were performed using a universal testing machine and equipment produced to realise three-point bending tests. Specifically, the test configuration consisted of a three-point bending test with a span of about 100 mm (Figure 5). In particular, the diameters of the support were equal to 8 mm, while the punch diameter was fixed to 10 mm. For completeness, the imposed crosshead speed was equal to 2 mm/min during the tests.
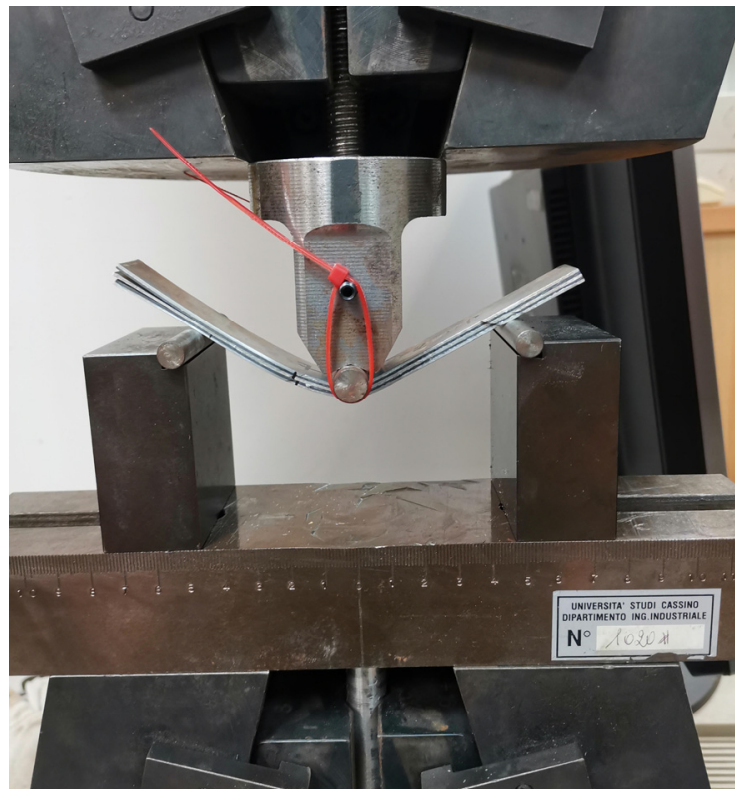

Figure 5. The three-point bending test of a specimen during testing and its deflection/deformation.

3. Results

The first results obtained from the analyses were related to the weight variations of the specimens at the end of each ageing stage. The obtained values of cwv_{Ref} and cwv_n are reported in Figures 6 and 7, respectively. Observing Figure 6, it is possible to state that saltwater was uptaken into the specimens, allowing an increase in weight of about 8%. This increase in weight was also due to the formation of salt crystals on the free surfaces of the specimens. The subsequent ageing stages allowed a reduction in weight of about 10%, reducing the weight of each sample to a value lower than the reference one. This result could be due to the microcracking of the composite matrix, the corrosion of the aluminium in saltwater, and the subsequent solution of salt crystals and aluminium oxides in the distilled water.

During the three-point bending test, crack propagation between the adhesive and aluminium sheets was observed. The failure modes can be classified according to ASTM

D5573 [29]. Here, the failure modes can be subdivided into six types: adhesive failure, if the failure appeared at the adhesive–adherend interface; cohesive failure, if the separation appeared within the adhesive itself; thin layer cohesive failure, if the failure appeared very near the adhesive–adherend interface with the presence of traces of FRP adherends on the adhesive; fibre tear failure, if the rupture appeared only in the FRP matrix with the exposure of the fibres on the failure surface; light fibre tear failure, if the rupture was in the FRP matrix near the bonded surface; stock break failure, if the failure appeared outside the bonded region. Starting from the observation of all the failure surfaces, it is possible to classify the failure mode obtained from testing as an adhesive failure for all the ageing conditions. Specifically, failures appeared between the adhesive and the outer aluminium sheets. It is possible to state that the interface between the adhesive and CFRP was optimal, while the interface between the adhesive and aluminium was the most-critical. Figure 8 shows the representative load–displacement curves obtained from the experimental tests. It is possible to observe that all the ageing conditions caused a decrease in mechanical performance, but contrary to what one might think, the last and the second to last ageing stage involved an increase in the mechanical performance with respect to the first stage of the ageing treatment. This could be due to a possible effect of the high temperature used for the thermal shock, which could allow for a post-cure effect on the adhesive and the composite layer. The presence of a working environment with higher temperatures during the last two stages of the ageing cycle could have a positive effect on the mechanical resistance of the specimens by a revamping of the physical ageing accumulated during the first stage of the aging cycle [10]. Moreover, the immersion in distilled water during the last two ageing stages resulted in a reduction in the salt content deposited within the specimens. In fact, while the saltwater-aged samples showed, in addition to a noticeable increase in weight, also the presence of salt crystals spread over the entire free surface of the aluminium, the specimens that were subsequently subjected to immersion in distilled water showed, in addition to a weight reduction lower than the initial reference one, also a clear reduction of the salt crystals on the free surface of the aluminium.
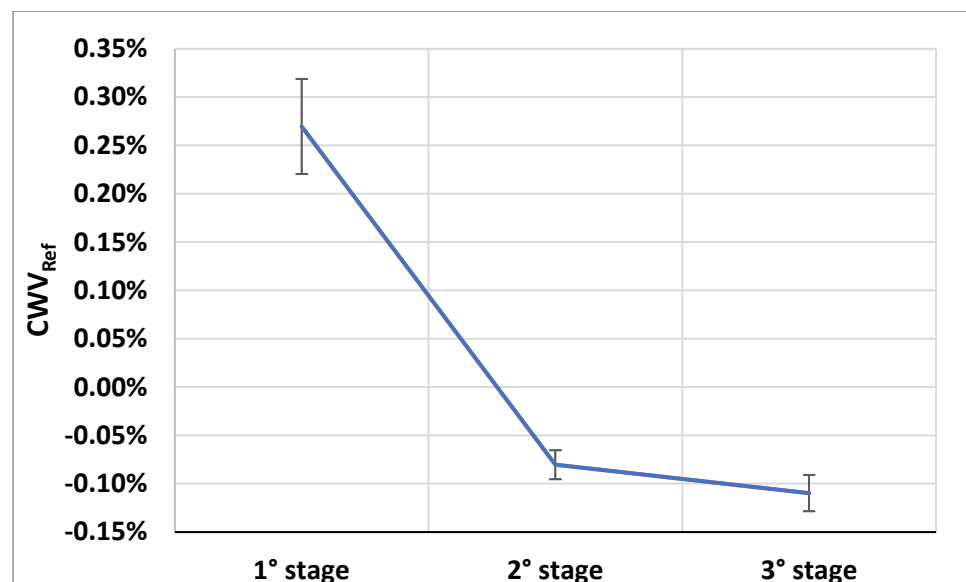

Figure 6. Coefficient of variations with respect to the unaged condition for each ageing stage.

Observing the maximum load obtained from the tests (Figure 9), it is possible to state that the average maximum load was lower, particularly for specimens aged only in saltwater at room temperature. Considering also the dispersion of the results, it is possible to state that the mechanical resistance variations were negligible compared to the other stages, despite the last stage showing a higher distribution. A decrease in the interfacial fracture energy in Ti-CFRP FMLs was also found by Yu et al. [14]. In particular, they aged

in simulated seawater both common and pre-treated laminates and found a decrease of 67% of the interfacial energy in the former case, while it was of 62% and 43% in the other cases. This decrement of the mechanical properties was induced by the hydration of the metal oxide layer, which had poor bonding with the composite matrix, and by the penetration of water into the matrix. Alia et al. [12] determined a decrease in the mechanical properties of adhesives equal to 25% due to microstructural changes induced by the hydrolytic action of the water. Pan et al. [20] found a decrease in the interlaminar shear of an aluminium-based FML equal to 14% after 15 days of hygrothermal ageing in seawater and 26% after 90 days.
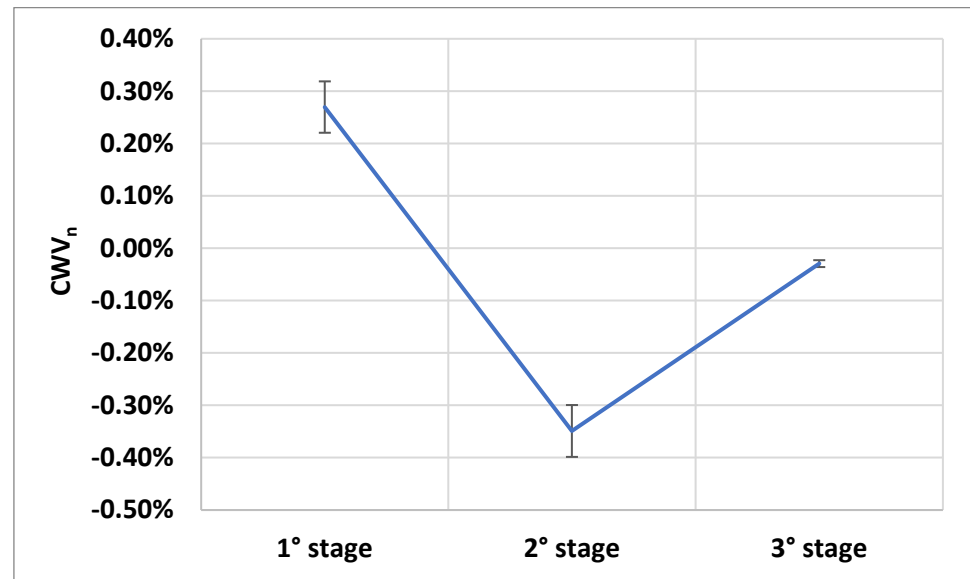

Figure 7. Coefficient of weight variation with respect to the previous ageing stage for each ageing stage.
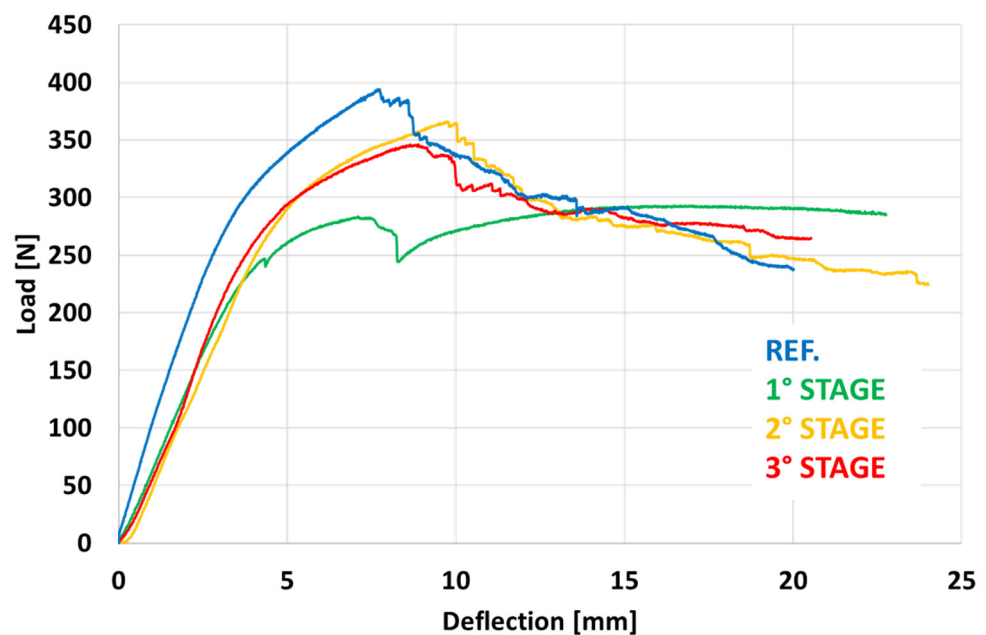

Figure 8. Average load–displacement curves obtained from the experimental tests.
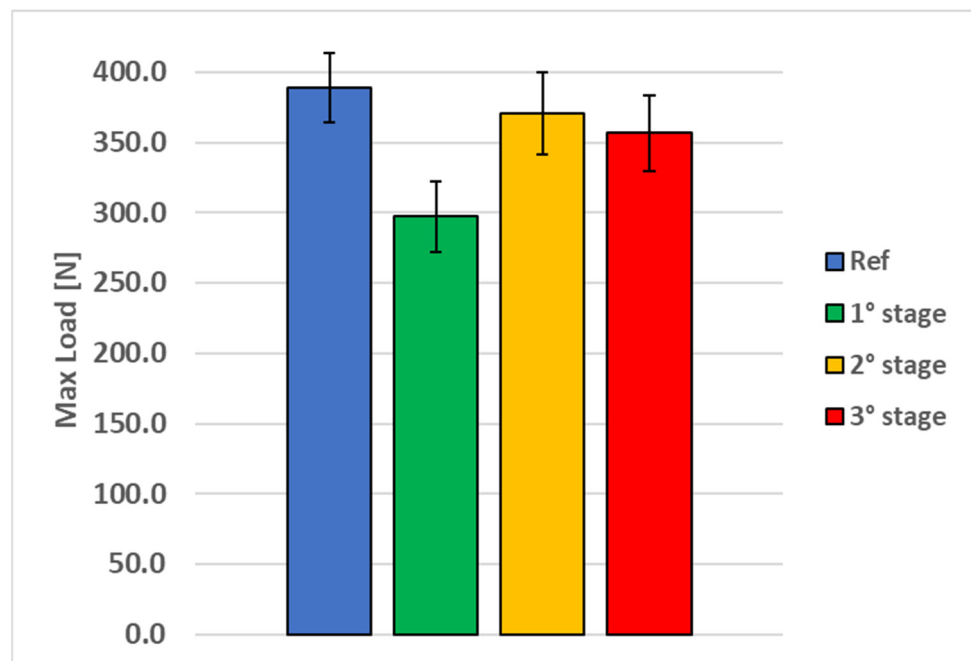
Figure 9. Maximum loads obtained from the experimental test (as a function of the ageing stage).

The observed variation in failure loads probably depended on the presence of salt crystals on the metal surfaces of the specimens. To understand this, the failure surfaces between the aluminium and composite were observed by optical microscope. Figure 10 shows the failure surfaces near the notch tip of a specimen aged only with the first stage, which was in saltwater. At the notch tip, it is possible to observe an extensive formation of salt crystals, which was not only concentrated at the notch apex, represented by the blue line, but developed within the bonding at the interface between the aluminium sheet and the adhesive. In fact, salt crystals at the notch tip were grown not only along the free surface of the aluminium, but also in the transverse direction. Such a phenomenon probably generated some peeling stress, which caused the crack propagation at the adhesive–aluminium interface. The free surface generated by this propagation led to a growth of salt crystals on the aluminium side (Figure 10c), which increased this phenomenon. The subsequent stages of ageing in distilled water involved a dissolution of salt crystals, therefore a decrease in the peeling stress at the crack tip and a consequent recovery of the mechanical performance of the FML specimens. It is likely that the surface pretreatment applied to the aluminium did not guarantee the performance needed to avoid the debonding between the aluminium and film adhesive. The analysis of the effect of different surface treatments on the aluminium sheets in these ageing conditions will be the subject of further work by the authors.
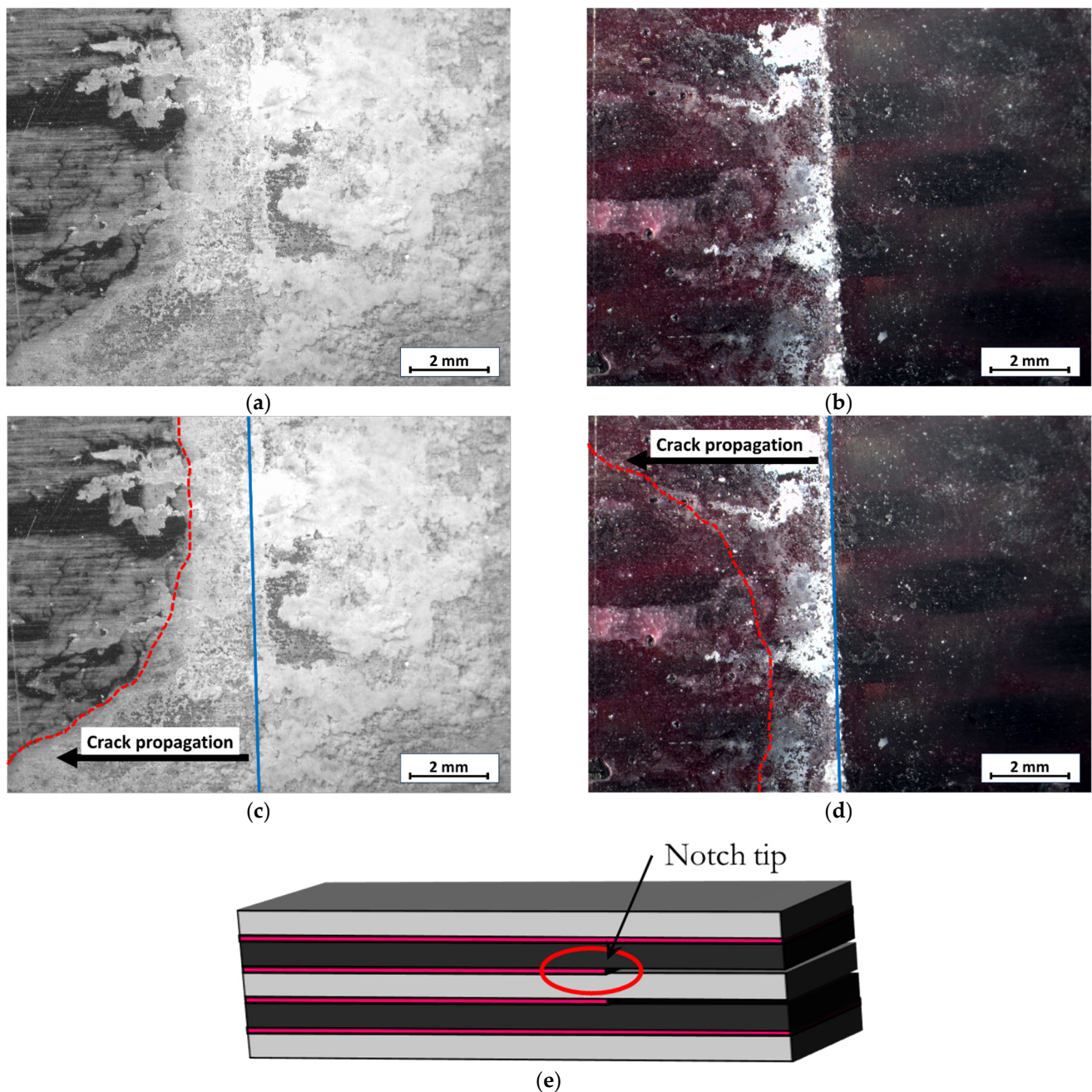
Figure 10. Failure surfaces of a specimen subjected to the first stage of ageing (saltwater): (**a**) salt crystals on the aluminium side; (**b**) salt crystal deposition on the adhesive side; (**c**) crack propagation on the aluminium side; (**d**) crack propagation on the adhesive side; (**e**) position of the region shown in the previous images.

4. Conclusions

In this work, the effect of ageing conditions on the mechanical performance of end-notched Fibre Metal Laminate (FML) specimens was investigated. The samples were manufactured through the vacuum bag technique and subjected to ageing cycles, which consisted of immersion in saltwater followed by thermal shocks in distilled water. At the end of each ageing cycle, the specimens were removed from the ageing environment, weighed, and tested through three-point bending tests. Specifically, the gravimetric analyses showed an increase in the weight of the specimens immersed in saltwater and a decrease in the weight in the subsequent ageing conditions in distilled water. This was due to the nucleation and growth of salt crystals on the free surfaces of the aluminium, which was

severely limited by the dissolution of the crystals in the distilled water in the subsequent ageing stages. After the gravimetric analyses, mechanical testing was performed, and the results showed a decrease in the failure loads of about 30% for the specimens aged in saltwater, while the subsequent ageing in distilled water showed a recovery of mechanical performance. This was probably due to an imperfect pretreatment of the aluminium surface before bonding and to the formation and growth of salt crystals near the crack tip, which allowed the concentration of peel stress and was removed by the dissolution of the salt crystals during the subsequent ageing stage in distilled water. Moreover, the presence of a working environment with higher temperatures during the last two stages of the ageing cycles could have an effect on the resistance of the specimens by a revamping of the physical ageing accumulated during the first stage of aging. Future works will investigate the effect of different aluminium surface pretreatments on the reliability of FML specimens in the same ageing conditions.

References

1. Stoll, M.; Stemmer, F.; Ilinzeer, S.; Weidenmann, K.A. Optimization of Corrosive Properties of Carbon Fiber Reinforced Aluminum Laminates Due to Integration of an Elastomer Interlayer. *Key Eng. Mater.* **2017**, *742*, 287–293. [CrossRef]
2. Li, X.; Zhang, X.; Zhang, H.; Yang, J.; Nia, A.B.; Chai, G.B. Mechanical Behaviors of Ti/CFRP/Ti Laminates with Different Surface Treatments of Titanium Sheets. *Compos. Struct.* **2017**, *163*, 21–31. [CrossRef]
3. Bellini, C.; Di Cocco, V.; Iacoviello, F.; Sorrentino, L. Experimental Analysis of Aluminium/Carbon Epoxy Hybrid Laminates under Flexural Load. *Frat. Ed Integrità Strutt.* **2019**, *13*, 739–747. [CrossRef]
4. Campilho, R.D.S.G.; da Silva, L.F.M.; Banea, M.D. Adhesive Bonding of Polymer Composites to Lightweight Metals. In *Joining of Polymer-Metal Hybrid Structures: Principles and Applications*; Wiley: New York, NY, USA, 2018; pp. 29–59. ISBN 9781119429807.
5. Bellini, C.; Di Cocco, V.; Sorrentino, L. Interlaminar Shear Strength Study on CFRP/Al Hybrid Laminates with Different Properties. *Frat. Ed Integrità Strutt.* **2019**, *14*, 442–448. [CrossRef]
6. Botelho, E.C.; Costa, M.L.; Pardini, L.C.; Rezende, M.C. Processing and Hygrothermal Effects on Viscoelastic Behavior of Glass Fiber/Epoxy Composites. *J. Mater. Sci.* **2005**, *40*, 3615–3623. [CrossRef]
7. Bellini, C.; Parodo, G.; Sorrentino, L. Effect of Operating Temperature on Aged Single Lap Bonded Joints. *Def. Technol.* **2020**, *16*, 283–289. [CrossRef]
8. Gibhardt, D.; Buggisch, C.; Meyer, D.; Fiedler, B. Hygrothermal Aging History of Amine-Epoxy Resins: Effects on Thermo-Mechanical Properties. *Front. Mater.* **2022**, *9*, 826076. [CrossRef]
9. Odegard, G.M.; Bandyopadhyay, A. Physical Aging of Epoxy Polymers and Their Composites. *J. Polym. Sci. Part B Polym. Phys.* **2011**, *49*, 1695–1716. [CrossRef]
10. Lee, J.K.; Hwang, J.Y.; Gillham, J.K. Erasure below Glass-Transition Temperature of Effect of Isothermal Physical Aging in Fully Cured Epoxy/Amine Thermosetting System. *J. Appl. Polym. Sci.* **2001**, *81*, 396–404. [CrossRef]
11. Botelho, E.C.; Almeida, R.S.; Pardini, L.C.; Rezende, M.C. Elastic Properties of Hygrothermally Conditioned Glare Laminate. *Int. J. Eng. Sci.* **2007**, *45*, 163–172. [CrossRef]
12. Alia, C.; Biezma, M.V.; Pinilla, P.; Arenas, J.M.; Suárez, J.C. Degradation in Seawater of Structural Adhesives for Hybrid Fibre-Metal Laminated Materials. *Adv. Mater. Sci. Eng.* **2013**, *2013*, 869075. [CrossRef]
13. Ali, A.; Pan, L.; Duan, L.; Zheng, Z.; Sapkota, B. Characterization of Seawater Hygrothermal Conditioning Effects on the Properties of Titanium-Based Fiber-Metal Laminates for Marine Applications. *Compos. Struct.* **2016**, *158*, 199–207. [CrossRef]
14. Yu, B.; He, P.; Jiang, Z.; Yang, J. Interlaminar Fracture Properties of Surface Treated Ti-CFRP Hybrid Composites under Long-Term Hygrothermal Conditions. *Compos. Part A Appl. Sci. Manuf.* **2017**, *96*, 9–17. [CrossRef]

15. Ostapiuk, M.; Bieniaś, J.; Surowska, B. Analysis of the Bending and Failure of Fiber Metal Laminates Based on Glass and Carbon Fibers. *Sci. Eng. Compos. Mater.* **2018**, *25*, 1095–1106. [CrossRef]

16. Rajan, B.M.C.; Kumar, A.S. The Influence of the Thickness and Areal Density on the Mechanical Properties of Carbon Fibre Reinforced Aluminium Laminates (CARAL). *Trans. Indian Inst. Met.* **2018**, *71*, 2165–2171. [CrossRef]

17. Mamalis, D.; Obande, W.; Koutsos, V.; Blackford, J.R.; Brádaigh, C.M.Ó.; Ray, D. Novel Thermoplastic Fibre-Metal Laminates Manufactured by Vacuum Resin Infusion: The Effect of Surface Treatments on Interfacial Bonding. *Mater. Des.* **2019**, *162*, 331–344. [CrossRef]

18. Romli, N.K.; Rejab, M.R.M.; Bachtiar, D.; Siregar, J.; Rani, M.F.; Salleh, S.M.; Merzuki, M.N.M. Failure Behaviour of Aluminium/CFRP Laminates with Varying Fibre Orientation in Quasi-Static Indentation Test. *IOP Conf. Ser. Mater. Sci. Eng.* **2018**, *319*, 012029. [CrossRef]

19. Wang, S.; Cao, M.; Wang, G.; Cong, F.; Xue, H.; Meng, Q.; Uddin, M.; Ma, J. Effect of Graphene Nanoplatelets on Water Absorption and Impact Resistance of Fibre-Metal Laminates under Varying Environmental Conditions. *Compos. Struct.* **2022**, *281*, 114977. [CrossRef]

20. Pan, L.; Ali, A.; Wang, Y.; Zheng, Z.; Lv, Y. Characterization of Effects of Heat Treated Anodized Film on the Properties of Hygrothermally Aged AA5083-Based Fiber-Metal Laminates. *Compos. Struct.* **2017**, *167*, 112–122. [CrossRef]

21. Hamill, L.; Hofmann, D.C.; Nutt, S. Galvanic Corrosion and Mechanical Behavior of Fiber Metal Laminates of Metallic Glass and Carbon Fiber Composites. *Adv. Eng. Mater.* **2018**, *20*, 1700711. [CrossRef]

22. Viandier, A.; Cramer, J.; Stefaniak, D.; Schröder, D.; Krewer, U.; Hühne, C.; Sinapius, M. Degradation Analysis of Fibre-Metal Laminates under Service Conditions to Predict Their Durability. *UPB Sci. Bull. Ser. D Mech. Eng.* **2016**, *78*, 49–58.

23. Hu, Y.; Li, H.; Fu, X.; Zhang, X.; Tao, J.; Xu, J. Hygrothermal Characterization of Polyimide-Titanium-Based Fibre Metal Laminate. *Polym. Compos.* **2018**, *39*, 2819–2825. [CrossRef]

24. Hu, Y.; Liu, C.; Wang, C.; Fu, X.; Zhang, Y. Study on the Hygrothermal Aging Behavior and Diffusion Mechanism of Ti/CF/PMR Polyimide Composite Laminates. *Mater. Res. Express* **2020**, *7*, 076508. [CrossRef]

25. Zhang, Y.; Wei, J.; Liu, C.; Hu, Y.; She, F. Reduced Graphene Oxide Modified Ti/CFRP Structure-Function Integrated Laminates for Surface Joule Heating and Deicing. *Compos. Part A Appl. Sci. Manuf.* **2023**, *166*, 107377. [CrossRef]

26. Bellini, C.; Di Cocco, V.; Iacoviello, F.; Sorrentino, L. Numerical Model Development to Predict the Process-Induced Residual Stresses in Fibre Metal Laminates. *Forces Mech.* **2021**, *3*, 100017. [CrossRef]

27. *ASTM D7905/D7905M-19e1*; Standard Test Method for Determination of the Mode II Interlaminar Fracture Toughness of Unidirectional Fiber-Reinforced Polymer Matrix Composites. ASTM International: West Conshohocken, PA, USA, 2019. [CrossRef]

28. *ASTM D1141-98*; Standard Practice for Preparation of Substitute Ocean Water. ASTM International: West Conshohocken, PA, USA, 2021. [CrossRef]

29. *ASTM D5573-99*; Standard Practice for Classifying Failure Modes in Fiber-Reinforced-Plastic (FRP) Joints. ASTM International: West Conshohocken, PA, USA, 2019. [CrossRef]